

Slow Dynamics of the Amphibian Tympanic Membrane

Christopher Bergevin*, Sebastiaan W.F. Meenderink[†], Marcel van der Heijden** and Peter M. Narins[‡]

^{*}*Department of Physics & Astronomy, York University, Canada*

[†]*Department of Physics and Astronomy, University of California, Los Angeles, California, USA*

^{**}*Department of Neuroscience, Erasmus MC, Rotterdam, The Netherlands*

[‡]*Department of Integrative Biology and Physiology, University of California, Los Angeles, California, USA*

Abstract.

Several studies have demonstrated that delays associated with evoked otoacoustic emissions (OAEs) largely originate from filter delays of resonant elements in the inner ear. However, one vertebrate group is an exception: Anuran (frogs and toads) amphibian OAEs exhibit relatively long delays (several milliseconds), yet relatively broad tuning. These delays, also apparent in auditory nerve fiber (ANF) responses, have been partially attributed to the middle ear (ME), with a total forward delay of ~ 0.7 ms (~ 30 times longer than in gerbil). However, ME forward delays only partially account for the longer delays of OAEs and ANF responses. We used scanning laser Doppler vibrometry to map surface velocity over the tympanic membrane (TyM) of anesthetized bullfrogs (*Rana catesbeiana*). Our main finding is a circularly-symmetric wave on the TyM surface, starting at the outer edges of the TyM and propagating inward towards the center (the site of the ossicular attachment). This wave exists for frequencies ~ 0.75 -3 kHz, overlapping the range of bullfrog hearing (~ 0.05 -1.7 kHz). Group delays associated with this wave varied from 0.4 to 1.2 ms and correlated with TyM diameter, which ranged from ~ 6 -16 mm. These delays correspond well to those from previous ME measurements. Presumably the TyM waves stem from biomechanical constraints of semi-aquatic species with a relatively large tympanum. We investigated some of these constraints by measuring the pressure ratio across the TyM (~ 10 -30 dB drop, delay of ~ 0.35 ms), the effects of ossicular interruption, the changes due to physiological state of TyM ('dry-out'), and by calculating the middle-ear input impedance. In summary, we found a slow, inward-traveling wave on the TyM surface that accounts for a substantial fraction of the relatively long otoacoustic and neurophysiological delays previously observed in the anuran inner ear.

INTRODUCTION

A long-standing question in auditory physiology has been the existence of substantial delays in the amphibian ear. These delays have been demonstrated to arise at both the neurophysiological [7] and otoacoustic levels [1, 11], yet appear unassociated with tuning [9, 15] as demonstrated for many other classes of land vertebrates. A recent review [4] recapitulated data from a previous study [10] and demonstrated that a significant fraction of this delay in the amphibian ear arises at the level of the middle ear, the tympanic membrane (TyM) in particular, and not at the level of the inner ear. However, the precise origin of this delay remained unclear. The present study sought to investigate the basis for this lag by examining the velocity profile across the surface of the TyM.

METHODS

We used adult American bullfrogs (*Rana catesbeiana*, 3 female and 1 male; Fig.1A) to record the vibration patterns of the TyM under free-field conditions. After induction of anesthesia (*i.p.* injection of pentobarbital; effective dosage: ~ 150 mg/kg), the animal was placed in the inside a double-walled sound-attenuating chamber. A scanning laser Doppler vibrometer (Polytec, Germany, PSV-300) allows vibration velocity to be measured (for successive stimulus presentations) along a user-specified grid (e.g., Fig.1B). A probe tube microphone (Sokolich) was positioned near (1–2 mm) the tympanic annulus to serve as a reference. Acoustic stimulation was delivered via a loudspeaker placed approximately 18 cm away from the TyM. Stimuli consisted of flat-voltage frequency sweeps repeated once every second. The duration of each FM sweep was 700 ms, during which the frequency changed linearly from 0.2 to 8 kHz (sweep rate ≈ 11.1 Hz/ms). Stimulus generation and data acquisition were controlled by Polytec software; subsequent analysis was done using customized software written in MATLAB.

Analysis was performed independently using two different methods. Both approaches assumed linearity and led to similar conclusions, though the second provided improved handling of noise. The first (Fig.1C) used Fourier

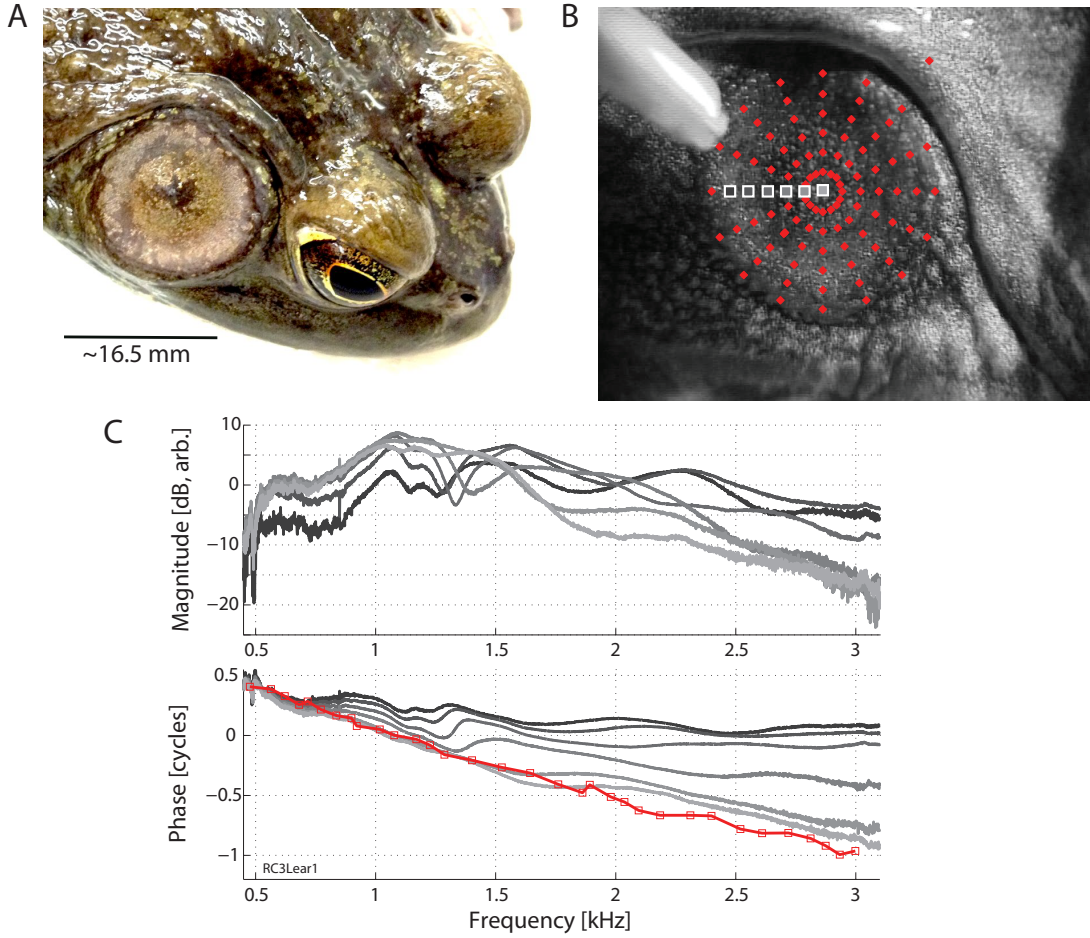


FIGURE 1. A. Large male bullfrog. Note that the TyM is relatively large, flush with side of head, and the surface is moist. The ossicular (i.e., columella) attachment point is at the center (dark spot). Females are relatively smaller (e.g., TyM diameter of approximately 7 mm). B. Female bullfrog, along with scanning grid (red diamonds). Note that the microphone is visible, placed $\sim 1 - 2$ mm away from TyM. C. TyM velocity at points shown in B (white squares correlate to each curve; darker means closer to TyM edge) referenced to nearby microphone. Magnitudes are in dB (arbitrary units). Traces are representative: Different radii and different frogs yielded comparable results. For comparison, red curve/squares indicate previously reported data for female bullfrog TyM motion (center re nearby microphone) [4, 10].

transforms, while the second (Figs. 2 and 3) used a more sophisticated strategy described briefly. To estimate the relevant transfer functions, the recorded time signal was bandpass filtered (0.15–10 kHz) and converted to a complex analytic signal $Z_{Resp}(t)$. From the parameters of the FM sweep (instantaneous frequency $f(t)$ and starting phase ϕ_0) the analytic version of the stimulus, $Z_{Stim}(t)$, was constructed:

$$Z_{Stim}(t) = \exp \left(i\phi_0 + 2\pi i \int_0^t f(t) dt \right) \quad (1)$$

Let the system have complex transfer function $H(f)$, then, for sufficiently slow sweeps, the response at any time t is related to the stimulus through multiplication by the “instantaneous transfer function” $H(f(t))$:

$$Z_{Resp}(t) = H(f(t))Z_{Stim}(t) \quad (2)$$

The instantaneous transfer function $H(f(t))$ was obtained by inverting eq. (2), followed by lowpass filtering (cutoff 250 Hz) to ensure that only temporally relevant portions of the sweeps (*i.e.*, the times t for which $f \cong f(t)$) contribute

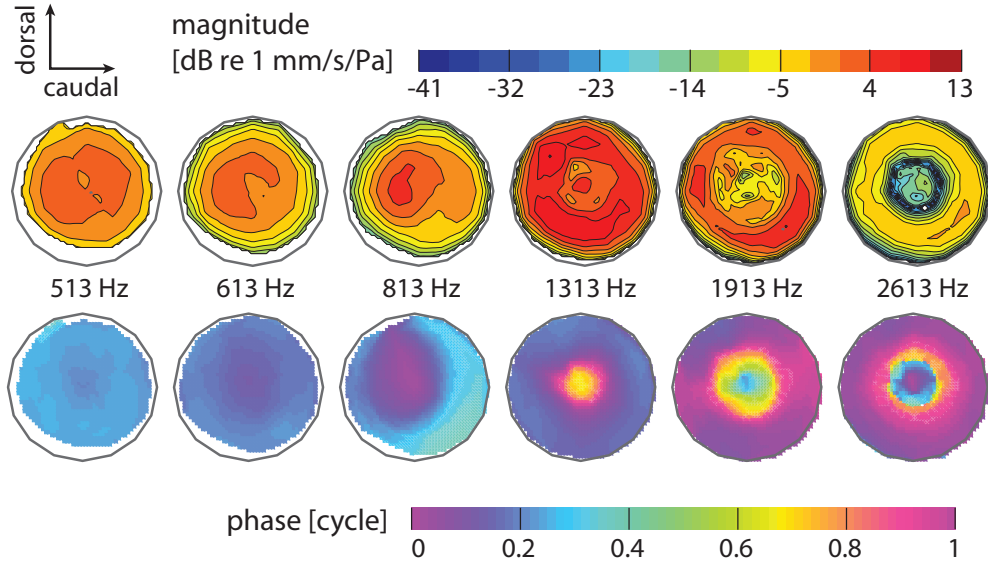


FIGURE 2. Magnitude (top row) and phase (bottom row) of TyM vibration at six different arbitrary frequencies. Data are referenced to the sound pressure next to the TyM. Each plot shows interpolated results from a maximum of 97 laser scan points; only data that exceeded the noise floor by at least 6 dB are included. The gray border indicates the largest circle (diameter: 8.4 mm) of scan points, and corresponds to the edge of the TyM.

to $H(f)$. Group delays (Fig. 3) in a given frequency band were estimated by a temporal method in which the transfer function $H(f)$ was used as a filter. A complex analytic 5-second Gaussian noise band $N(t)$, having center frequency CF and bandwidth BW was computed and passed through the filter associated with $H(f)$, resulting in filtered noise band $N_F(t)$. The group delay was then determined by cross-correlating the squared envelopes (i.e., instantaneous power) of $N(t)$ and $N_F(t)$ and locating the peak. This was done for each pair of TyM locations and between the acoustic recording and each TyM location, leading to an overdetermined set of linear equations of the type $\tau_i - \tau_j = \tau_{ij}$, with τ_{ij} the relative group delays from cross-correlation and τ_i the desired individual group delays. After rejecting τ_{ij} originating from peaks having a normalized cross-correlation smaller than 0.9, the τ_i were determined by solving the equations using least-squares (c.f. Eqn.3 in [6]) while setting the group delay of the acoustic waveform to 0 ms.

RESULTS

Motion. Significant phase accumulation (relative to the microphone) was apparent progressing from the outer rim of the TyM towards the center (Fig. 1C), indicating a delay between TyM velocity and acoustic stimulus and suggestive of a slow inward-traveling wave. Similar results were observed for different radial tracks and frogs, though more phase accumulation was apparent for the male frog with a relatively larger TyM diameter. Overall, the present data appear consistent with previous measurements of frog TyM motion [4, 10, 13].

Figure 2 shows the magnitude and phase of TyM vibration at six different frequencies. First, the response of the TyM is more or less radially symmetrical, independent of stimulus frequency. Second, the vibration pattern changes with stimulus frequency. For low stimulus frequencies (513 Hz in Fig.2), the TyM vibrates in (0,1) mode: The entire membrane moves in phase, with a single circular node (at the edge) and maximum velocity near the center of the TyM. As frequency increases this pattern changes, and radial phase differences become apparent, suggestive of a traveling-wave pattern. Eventually, the center (i.e., place of ossicular attachment) moves less at higher frequencies and intermediate nodes become apparent (e.g., 2613 Hz), suggestive of standing waves.

Delay. Estimates of the group delay for a representative ear/frequency range are shown in Fig.3. The lower row is not ordered according to significance; the group delay is effectively filtered by the requirement of power-correlations (see Methods) of at least 0.9 with any other location. Similar results are found for other ears/frequency ranges, though evidence for standing waves was sometimes apparent. Overall, the data suggest a TyM edge-to-center group delay of 0.3-0.8 ms for the female frogs, longer for the large male.

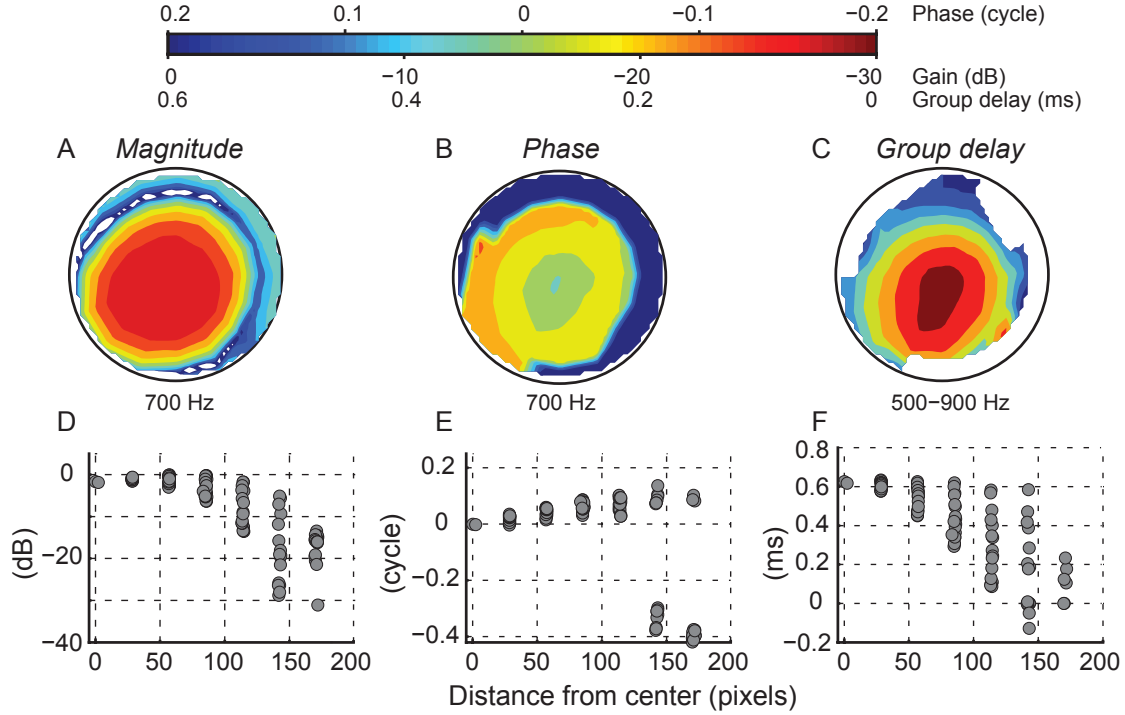


FIGURE 3. Representative example of motion and associated estimated delays from a female bullfrog. Upper row shows spatial maps of: (A) vibration magnitude; (B) phase; (C) group delay, each of them referenced to the microphone recording. The color coding for these 3 maps is given by a single colorbar with 3 separate sets of tick labels. The bottom row (D-F) plots the corresponding data as a function of distance from TyM center.

Additional observations. Several other measurements were made that are described briefly here. First, advancing the microphone across the TyM face revealed little variation (≤ 1 dB) below 4 kHz, indicating uniform stimulation. Second, in several ears an additional microphone (Etymotic ER-7) was placed inside the middle ear cavity near the TyM such that the pressure difference across the TyM could be measured. A pressure drop was apparent (10-30 dB), with the largest drops below ~ 1.5 kHz. The phase suggested a delay of roughly 0.35 ms, consistent with the TyM group delays. Third, in several ears the effects of ‘dry out’ was measured by leaving the frog (postmortem) in place overnight. Overall, there was a shift towards higher frequencies and velocity magnitudes decreased substantially, as did the phase accumulation. Lastly, the effects of disarticulation were examined by visibly interrupting the collumellar connection between TyM and inner ear. Overall, there was no drastic change in phase behavior upon disarticulation, though the magnitude response was more complex.

DISCUSSION

Physical interpretation. While the overall bullfrog TyM motion is complex, we propose a relatively simple model to capture its essential features. Consider the TyM as a distributed segment of transmission line (e.g., [12]) connecting the air to the ossicles (and subsequently the inner ear). At frequencies where the characteristic impedance of the transition (i.e., air-to-TyM, TyM-to-ossicle) is well-matched, a slow-traveling wave behavior will dominate. Mismatch can cause reflections and thereby standing waves.

Connection to mammalian TyM motion. The mammalian TyM is known to undergo complex motion [5, 16], yet many questions remain about the basis for how the mammalian TyM provides such efficient and uniform energy transfer over so wide a frequency range. Certain mammalian middle ear models have considered the TyM to behave as a transmission line that causes a delay of approximately $40 \mu\text{s}$ [14]. However, it is unclear if direct physiological measurements of TyM motion are consistent with such a framework, as there is not always clear evidence for an inward-traveling wave carrying energy to the inner ear [2, 3, 8]. We note that the delays observed here for the bullfrog

TyM are consistent with delays observed at the level of the inner ear [4, 7] and are approximately an order of magnitude longer than those observed for mammalian middle ear delay for animals such as the gerbil.

Presumably the biomechanical basis for the relatively long delays of the bullfrog TyM (Fig.1A) stems from numerous factors, such as: the overall diameter (5-20 mm), relative thickness, superficial mucosal nature (associated with the animal's amphibious nature), and relative flatness (compared to the more conical nature of the mammalian TyM). Finite element models may help elucidate which of these aspects (or others) cause TyM motion to differ between amphibians and terrestrial vertebrates (e.g., most mammals).

ACKNOWLEDGMENTS

Supported by the Natural Sciences and Engineering Research Council of Canada (NSERC). We thank Dolores Bozovic for assistance. All animal care adhered to the ABS Guidelines for the use of animals in research and was approved by the UCLA Animal Research Committee (Protocol # 094-086-62).

REFERENCES

- [1] Bergevin C, Freeman DM, Saunders JC, Shera CA (2008) Otoacoustic emissions in humans, birds, lizards, and frogs: evidence for multiple generation mechanisms. *J Comp Physiol A* 194:665–683
- [2] Bergevin C, Olson ES (2014) External and middle ear sound pressure distribution and acoustic coupling to the tympanic membrane. *J Acoust Soc Am* 135:1294–1312
- [3] Cheng JT, Hamade M, Merchant SN, Rosowski JJ, Harrington E, Furlong C (2013) Wave motion on the surface of the human tympanic membrane: Holographic measurement and modeling analysis. *J Acoust Soc Am* 133:918–937
- [4] van Dijk P, Mason MJ, Schoffelen RLM, Narins PM, Meenderink SWF (2011) Mechanics of the frog ear. *Hear Res* 273:46–58
- [5] Fay JP, Puria S, Steele CR (2006) The discordant eardrum. *Proc Nat Acad Sci Am* 103:19743–19748
- [6] van der Heijden M, Joris PX (2003) Cochlear phase and amplitude retrieved from the auditory nerve at arbitrary frequencies. *J Neurosci* 23:9194–9198
- [7] Hillery CM, Narins PM (1984) Neurophysiological evidence for a traveling wave in the amphibian inner ear. *Science* 225:1037–1039
- [8] de La Rochefoucauld O, Olson ES (2010) A sum of simple and complex motions on the eardrum and manubrium in gerbil. *Hear Res* 263:9–15
- [9] Lewis ER (1987) Speculations about noise and the evolution of vertebrate hearing. *Hear Res* 25:83–90
- [10] Mason MJ, Narins PM (2002) Vibrometric studies of the middle ear of the bullfrog *Rana catesbeiana* I. The extrastapes. *J Exp Biol* 205:3153–3165
- [11] Meenderink SWF, Narins PM (2006) Stimulus frequency otoacoustic emissions in the Northern leopard frog, *Rana pipiens pipiens*: Implications for inner ear mechanics. *Hear Res* 220:67–75
- [12] Parent P, Allen J (2007) Wave model of the cat tympanic membrane. *J Acoust Soc Am* 122:918–931
- [13] Pinder AC, Palmer AR (1983) Mechanical properties of the frog ear: Vibration measurements under free- and closed-field acoustic conditions. *Proc Roy Soc B: Biol Sci* 219:371–396
- [14] Puria S, Allen JB (1998) Measurements and model of the cat middle ear: evidence of tympanic membrane acoustic delay. *J Acoust Soc Am* 104:3463–3481
- [15] Ronken D (1991) Spike discharge properties that are related to the characteristic frequency of single units in the frog auditory nerve. *J Acoust Soc Am* 90:2428–2440
- [16] Tonndorf J, Khanna S (1972) Tympanic-membrane vibrations in human cadaver ears studied by time-averaged holography. *J Acoust Soc Am* 52:1221–1233